Current Pharmaceutical Design, 2018, *24*, 595-614

RESEARCH ARTICLE

Identification of the Multifaceted Chemopreventive Activity of Curcumin Against the Carcinogenic Potential of the Food Additive, $KBrO_3$

Ismael Obaidi[1,3,*], Michael Higgins[1], Bojlul Bahar[2], Jessica L. Davis[1] and Tara McMorrow[1]

[1]*UCD Centre for Toxicology, School of Biomedical and Biomolecular Sciences, Conway Institute, University College Dublin, Dublin, Ireland;* [2]*International Institute of Nutritional Sciences and Applied Food Safety Studies, University of Central Lancashire, Preston, PR1 2HE, United Kingdom;* [3]*School of Pharmacy, University of Babylon, Babylon, Iraq*

Abstract: ***Background***: Potassium bromate ($KBrO_3$), a food additive, has been used in many bakery products as an oxidizing agent. It has been shown to induce renal cancer in many *in-vitro* and *in-vivo* experimental models

Objectives: This study evaluated the carcinogenic potential of potassium bromate ($KBrO_3$) and the chemopreventive mechanisms of the anti-oxidant and anti-inflammatory phytochemical, curcumin against $KBrO_3$-induced carcinogenicity.

Method: Lactate dehydrogenase (LDH) cytotoxicity assay and morphological characteristics were used to assess curcumin's cytoprotective potential against $KBrO_3$ toxicity. To assess the chemopreventive potential of curcumin against $KBrO_3$-induced oxidative insult, intracellular H_2O_2 and the nuclear concentration of the DNA adduct 8-OHdG were measured. PCR array, qRT-PCR, and western blot analysis were used to identify dysregulated genes by $KBrO_3$ exposure. Furthermore, immunofluorescence was used to evaluate the ciliary loss and the disturbance of cellular tight junction induced by $KBrO_3$.

***Results*:** Oxidative stress assays showed that $KBrO_3$ increased the levels of intracellular H_2O_2 and the DNA adduct 8-OHdG. Combination of curcumin with $KBrO_3$ efficiently reduced the level of H_2O_2 and 8-OHdG while up-regulating the expression of catalase. PCR array, qRT-PCR, and western blot analysis revealed that $KBrO_3$ dysregulated multiple genes involved in inflammation, proliferation, and apoptosis, namely CTGF, IL-1, and TRAF3. Moreover, qRT-PCR and immunofluorescence studies showed that $KBrO_3$ negatively affected the tight junctional protein (ZO-1) and induced a degeneration of primary ciliary proteins. The negative impact of $KBrO_3$ on cilia was markedly repressed by curcumin.

***Conclusion*:** Curcumin could potentially be used as a protective agent against carcinogenicity of $KBrO_3$.

ARTICLE HISTORY

Received: November 16, 2017
Accepted: December 11, 2017

DOI:
10.2174/1381612824666171226143201

Keywords: Potassium bromate ($KBrO_3$), chemoprevention, curcumin, primary cilia, kidney cancer, inflammation.

1. INTRODUCTION

Potassium bromate ($KBrO_3$), a food additive, has been used in different bakery products as an oxidizing agent. In 2005, the use of $KBrO_3$ as a food additive was banned by countries of the European Union, Canada, Japan, China, India, and South America. Surprisingly, it has not been banned by the FDA in the US and still can be found in some bakery products [1, 2]. $KBrO_3$ was shown to induce renal cancer in many *in-vitro* and *in-vivo* experimental models [3-5]. Shiao *et al*. found that rats exposed to $KBrO_3$ in drinking water caused a mutation in the Von Hippel-Lindau tumor (VHL) gene, a crucial tumor suppressor that has been found to be mutated in renal cell carcinomas [6]. $KBrO_3$, was found to induce oxidative DNA damage and DNA adduct formation that lead to various gene mutations. For instance, the formation of the mutagenic 8-hydroxy deoxyguanosine (8-OHdG) was detected following the exposure of porcine kidney cells to $KBrO_3$ [7]. Interestingly, $KBrO_3$ was found to interact with GSH to form the highly reactive 8-oxodeoxyguanosine (8-oxodG), thus causing DNA double strand break [8, 9].

Following DNA damage, many genes including those controlling apoptosis and inflammation are dysregulated. For instance, Bader and Hsu mentioned that many pro-inflammatory genes such as HIF1a, HIF2a, TNF-α, TGF-β, and NF-KB were found to be up-regulated in response to DNA damage that eventually induced VHL mutation [10].

*Address correspondence to this author at the UCD Centre for Toxicology, School of Biomedical and Biomolecular Sciences, Conway Institute, University College Dublin, Dublin, Ireland;
E-mail: Ismael.obaidi@ucdconnect.ie

Primary cilia are immotile sensory organelles that play an important role in cell differentiation, polarity, and quiescence. They can receive mechanical and chemical signals from other cells as well as, from the surrounding environment [11]. Normally, cells assemble cilia on their membranes when they "stop" dividing, exit the cell cycle, and start to differentiate [12]. However, cells tend to lose cilia when they re-enter the cell cycle and mitosis [13]. In most renal cell carcinomas where the suppressor VHL gene is inactivated, Schraml *et al*. found that ciliary loss in clear cell renal cell carcinoma (ccRCC) was strongly associated with the mutation of this tumor suppression gene. In contrast, the author found that in papillary renal cell carcinomas, the frequency of cilia was higher than ccRCC and the ciliary loss was VHL independent, which points to the differences in the biological pattern between these types of cancer cells [14].

Chemoprevention is a novel aspect in cancer development and treatment referring to the use of natural, semi-synthetic or synthetic compounds to halt, stop, or reverse tumor formation and progression [15]. Chemopreventives can block tumor initiation; therefore, they are termed blocking agents. For instance, anti-oxidants, free radical scavengers, phase I drug-metabolizing enzymes inhibitors, and phase II drug-metabolizing enzymes inducers are deemed cancer blocking agents. Whereas compounds that halt the stages of tumor promotion and progression are referred to as tumor suppressors. Induction of apoptosis, terminal cell differentiation, inhibition of cell proliferation and clonal expansion, and alteration of gene expression of preneoplastic tumors are examples of tumor suppression [15-17].

1873-4286/18 $58.00+.00

Curcumin, also known as diferuloylmethane, is a polyphenolic compound derived from the root and rhizome of the plant Curcuma longa [18, 19]. Curcumin has a chemoprevention potential owing to its anti-oxidant, anti-inflammatory, immunomodulatory, and pro-apoptotic potential [20]. While curcumin abrogates several oncogenic pathways such as NF-KB, Akt/PI3K and MAPK, it has recently been found to induce anti-tumor potential via epigenetic modulations of critical genes. For instance, it dysregulates several oncogenic and tumor suppressor miRNAs, namely, miR-21, miR-17-5p, miR-22, miR-15a, miR-20a, and miR-27a [21, 22].

This study aimed at investigating the carcinogenic potential of $KBrO_3$ and the mechanisms by which curcumin can prevent the carcinogenic insults of $KBrO_3$ on the renal epithelial cells (RPTEC/TERT1). Moreover, our group has reported that targeting RPTEC/TERT1 with a subtoxic concentration of $KBrO_3$ was associated with loss of primary cilia [23], therefore this study also investigated the preventive potential of curcumin against $KBrO_3$ induced deciliation, and thus inhibited proliferation and dedifferentiation.

2. MATERIALS AND METHOD

2.1. Cell Culture and Treatment

The human renal proximal tubular epithelial (RPTEC/TERT1) [24] and ACHN cell lines were obtained from the American Tissue Culture Collection (ATCC). Cells were maintained in low glucose (5 mM) Dulbecco's Modified Eagle / Nutrient Mix F-12 medium supplemented with 5µg/ml insulin, 5µg/ml transferrin, 5µg/ml selenite (ITS), 36ng/ml hydrocortisone, 10ng/ml epidermal growth factor (EGF) (Sigma-Aldrich) 50 U/ml penicillin, 50µg/ml streptomycin (P/S), and 2mM L-glutamine (Gibco, Life Technologies). ACHN cells were maintained in Minimum Eagle Medium (Sigma-Aldrich) with 10% FBS and P/S. Both cell lines were incubated at 37^{o} C in a 5% CO_2 humidified atmosphere.

RPTEC/TERT1 were seeded at a density of $1x10^6$ cells/ml. Cells were maintained for 10 days after reaching 100% confluency to allow stabilization of the monolayer [23]. While ACHN cells were seeded at the same density one day in advance before the treatment. $KBrO_3$ and curcumin were purchased from (Sigma-Aldrich, Taufkirchen, Germany). $KBrO_3$ was dissolved in water to prepare 100mM stock solution which was then further diluted with culture medium to get the indicated concentrations. Curcumin and silymarin were dissolved in DMSO to prepare stock solutions of 250 mM and 50mM, respectively. They were then further diluted with culture medium to final concentration 200 µM and 25 µM, respectively. In most experiments, where curcumin or silymarin was used, control cells were exposed to a maximum 0.1% DMSO.

2.2. Lactate Dehydrogenase (LDH) Release Assay

The LDH assay was performed using a Roche kit (Roche Diagnostics, Mannheim, Germany). Briefly, RPTEC/TERT1 cells were cultured at density of $1x10^6$ cells/ ml in 24-well plates and allowed to form a fully confluent monolayer. 10 days post confluency, cells were treated with six different concentrations of $KBrO_3$ (0.5,1,2,3,5, and 10 mM) only or in a combination with 25µM curcumin for 24h. The positive control for maximum LDH release or 100% cell death was prepared by treating cells with 2% Triton-X 100 for 5 min at 37°C. Following 15min incubation of cell supernatants with the reaction mixture (provided by the kit), the absorbance was measured at 490nm using Spectamax2 plate reader (Molecular devices, Winnersh/ UK). LDH release was expressed as a percentage of the maximum LDH activity.

2.3. Phase Contrast Microscopy

RPTEC/TERT1 cells at $1x10^6$ cells/ ml were cultured in 24-well plates and allowed to form a fully confluent monolayer. 10 days post-confluency, cells were treated with $KBrO_3$ (10mM) only or in a combination with 25µM curcumin for 24h at 37°C. Cellular morphology was observed by phase contrast microscopy using a JVC high-resolution digital camera (KY-F55BE) attached to a Nikon TMS phase contrast microscope. Micrographs were processed using ImageJ v.1.49.

2.4. Determination of Intracellular H_2O_2 Concentration

Intracellular hydrogen peroxide (H_2O_2) concentrations were measured using Amplex red assay kit (Thermo Fisher scientific, Carlsbad, CA) following the manufacturer instructions. Briefly, cells were cultured in 12 well culture plates. Following treatment, cells were lysed in 200 µl ice-cold lysis buffer (0.1% Triton X-100 in 0.05 M sodium phosphate buffer, pH 7.4). Following this, lysates were transferred to pre-chilled microfuge tubes and vortexed every 3 min for 15 min for complete cell homogenization. Tubes were centrifuged at 14,000 g at 4°C for 15 min. A volume of 50 µl of supernatants and standard H_2O_2 solutions (0, 0.05, 0.1, 0.25, 0.5, 0.75, 1, 1.25, 2, and 5 µM) were loaded in 96-well opaque black microplate. An equal volume of Amplex Red reaction mixture (0.1 mM Amplex red reagent and 0.2 U/ml horseradish peroxidase in 1X reaction buffer) was added to the pre-loaded wells to initiate the reaction. The fluorescence was measured kinetically every 30 sec for 30 min at excitation and emission wavelengths of 530 and 590 nm, respectively using a scanning microplate reader (Molecular Devices Inc, Sunnyvale, CA, USA). Intracellular H_2O_2 concentration was calculated using the standard curve and normalized to the total protein content.

2.5. Determination of Intra-nuclear Concentration of 8-OHdG

This assay consists of 4 stages: DNA extraction, determination of DNA concentration, DNA digestion, and measuring the concentration of the DNA adduct 8-OHdG.

DNA was extracted from cells using WAKO DNA Extractor WB Kit (Wako, Osaka, Japan) which contains sodium iodide (NaI) as chaotropic agent to minimize the oxidation of DNA during the extraction. The concentrations of DNA solutions were calculated using the Thermo Fisher Scientific NanoDrop 2000 (Thermo Fisher Scientific, Wilmington, DE, USA). The Wako 8-OHdG Assay Preparation Reagent kit was used exclusively to digest DNA and release 8-OHdG. Determination of the intranuclear 8-OHdG concentration was performed using an enzyme-linked immunosorbent assay (ELISA) kit (Highly Sensitive 8-OHdG Check ELISA kit, Japan Institute for the Control of Aging, Fukuroi, Japan). Briefly, a volume of 50 µl of digested DNA samples and standard concentrations were loaded to the provided ELISA plate. A volume of 50 µl primary antibody per a well was added and incubated overnight at 4°C. Next day, the well contents were poured off and washed three times using 250µl/well washing solution. The wells were incubated with100 µl/ well of secondary antibody for 1h at room temperature. The plate was washed before adding a chromatic solution and incubated for 15 min at room temperature in a dark place. Finally, the reaction was terminated by adding 100µl of the reaction terminating solution. The absorbance was read at 450 nm.

2.6. Immunofluorescent Labeling

For immunofluorescent labeling experiments, cells were cultured in 8-well chamber slides (Millipore, USAand allowed to form a fully confluent monolayer. 10 days post-confluency, cells were treated with DMSO-containing medium, 5.5mM $KBrO_3$, 25µM curcumin, or a combination of both for 24h at 37 °C. Following treatment, cells were washed with PBS three times and fixed with 3.7% formaldehyde for 20 min at room temperature. Cells were then washed three times with PBS and permeabilized with 0.2%(v/v) Triton-X 100 in PBS. Background was reduced by blocking nonspecific signals with 0.5% (w/v) BSA in PBS. The ciliary markers Acetylated α-tubulin and Arl 13B were labeled using a mouse anti-human antibody (1:400) (Sigma-Aldrich, Taufkirchen,

Germany) and a rabbit anti-human antibody, respectively. ZO-1 was labeled using a rabbit anti-human antibody (1:300) (Zymed, Invitrogen, South San Francisco, CA). Nuclei were stained with Hoechst 33342 (1:1000) (Sigma-Aldrich, Taufkirchen, Germany). Slides were imaged using a Zeiss A-Plan 40X/0.65 objective and a Zeiss M1 Upright AxioImager with CoolLED P3000 light source or a Zeiss C-Plan-Apochromat 40X/1.3 objective and a Zeiss LSM510 UVMETA confocal microscope. Images were deconvolved using Auto Quant-X3 deconvolution software (Version 3.0.3) (Media Cybernetics Inc.) at 5 iterations. Images were adjusted for brightness and contrast using Fiji/ImageJ (Fiji.sc/).

2.7. RNA Extraction and Preparation of cDNA

RPTEC/TERT1 cells were seeded and treated as described earlier using 6-well plate format. TRIzol method was used to extract total RNA. The same method was applied to extract the total RNA from the ACHN cells after 24h of growth. Briefly, TRIzol (Life Technologies, USA) was used to lyse cells (1ml per a well). Cells were then homogenized by passing through pipette tip several times. Following the homogenization, 200µl of 1–bromo–3–chloropropane (BCP), a chloroform derivative, was added to the homogenate, mixed by vertexing, incubated for 3 min at room temperature, then centrifuged at 12,000 × g at 4°C for 15min. The mixture was separated into three phases: aqueous (RNA), interphase and a red lower organic layer (DNA and protein). The aqueous phase was transferred into a clean microfuge tubes then 500µl isopropanol was added to precipitate RNA. Following centrifugation at 12,000 × g at 4°C for 15 min, the supernatant was discarded and the pellets were washed with 500µl of 75% ethanol to remove further impurities. The microfuge tubes were finally centrifuged at 7500g at 4°C for 5 min. The supernatant was discarded and RNA pellets were dissolved in ddH_2O. For further RNA purification and removing of genomic DNA contamination, mRNeasy and DNase Max kit (Qiagen, UK) were used according to the manufacturer protocol. The yield of the RNA was assessed by measuring the optical density at 260 nm and 280nm using a Nanodrop ND-1000 spectrophotometer (Thermo Fisher Scientific, Wilmington, DE, USA). The purity of RNA samples was assessed based on the absorbance ratio of 260:280 which should be ≥1.8. A total RNA of 1µg was reversed transcribed to cDNA using a RevertAid H Minus First Strand cDNA synthesis Kit (Fermentas GmbH, St. Leon-Rot, Germany) according to the manufacturer's instructions.

2.8. Quantitative Real-Time PCR Analysis

Quantitative expression of a total of 192 genes (list of genes provided in the supplementary Table **1**) involved in inflammation, angiogenesis, and apoptosis were evaluated using real-time PCR ABI PRISM® 7900HT (Foster City, California USA). These were customized PCR arrays designed by (Sigma-Aldrich, Taufkirchen, Germany) Corp. For the PCR array experiment, 20µL cDNA of each individual treatment was diluted up to 170µL using distilled water. Three biological replicates of a single treatment group were pooled and analyzed. The real-time PCR mix (20µL/well) contained 1µL of pooled cDNA, 3µL water, 6µL primer mix, and 10µL SYBR green master mix. The thermal cycle conditions were 95°C for 15min followed by 45 cycles of 94°C for 15 sec, 55 °C for 30 sec, and 70 °C for 30 sec. The dissociation stage was set at 95 °C for 15 sec, 60°C for 15 sec, and 95°C for 15 sec, as previously described [25] The mRNA abundances were expressed in "cycle threshold" (Ct) values, which represents the number of PCR cycles after which the PCR product crosses a threshold value. A Ct value of 35 was used as the cut-off limit. The normalization of gene expression was carried out based on the abundance of the house-keeping genes βactin (*ACTB*), glyceraldehyde 3-phosphate dehydrogenase (*GAPDH*) and beta-glucuronidase (*GUSB*).

Validation of the PCR array was performed using single tube TaqMan-probe based gene expression assays (Applied Biosystems, Foster City, CA, USA). Normalization of genes expression was carried out using the house-keeping gene β-actin. The PCR reaction mixture (10µL) consisted of 0.5µL cDNA, 3.5µL nuclease free water, 0.5µL primer mix, 0.5µL loading control (β-actin), and 5µL TaqMan master mix. The thermal cycle conditions were as follows: 50°C for 2 min, 95 °C for 10 min followed by 40 cycles of 95 °C for 15 s, 60 °C for 1 min. Samples were loaded in an optical 384 well plate in duplicates (10µL/ well) and Ct values <35 were used as the cut-off limit. For the analysis of both PCR array and qRT-PCR, the $2^{-\Delta\Delta Ct}$ method was applied. Briefly, average ΔCt was calculated as the difference of Ct values of any target gene from the average of the Ct value of the reference gene (s). Then, fold change was calculated as $2^{(-\text{average } \Delta Ct \text{ target gene})/2(-\text{average } \Delta Ct \text{ reference gene})}$. A fold difference cut-off point was set at ≥2.0.

2.9. Western Blot Analysis

Western blot analysis was carried out according to the standard method by Buchmann [26]. Following cell treatment, the media was removed, and the cells were lysed by using RIPA buffer (Sigma-Aldrich, Taufkirchen, Germany). Total protein concentration was determined by Bradford method using BCA protein assay kit (Pierce, Rockford, IL, USA) according to the manufacturer protocol. Equal amounts of 20µg of whole cell lysates were placed in each lane and subject to SDS-PAGE electrophoresis, then transferred to a 0.2µm pore size Whatman Protran® nitrocellulose membrane (Thermo Fisher Scientific, Wilmington, DE, USA) using a semi-dry transfer system. After the transfer, the membranes were blocked by incubation with TBS-T buffer (50 mM tris-HCl, pH 7.4, 150 mM NaCl, and 0.05% Tween 20) containing 5% non-fat milk or BSA for 1hr at room temperature. The membranes were then incubated overnight at 4°C with CTGF primary antibody (1:1000) (Santa Cruz, USA) and GAPDH (1:10,000) (Cell Signaling Technology Inc, Danvers, MA, USA). Next day, the blots were washed with T-BST then incubated with TBS-T/ 5% non-fat milk containing an appropriate secondary antibodies coupled with horse radish peroxidase (HRP) (Cell Signaling Technology Inc, Danvers, MA, USA) for 1h at room temperature. Immunodetection was performed using the SuperSignal West Pico Substrate (Thermo Scientific, Rockford, IL, USA).

2.10. Statistical Analysis

All experiments were repeated at least three times. Statistical analyses were performed using Graph Pad Prism 5.0. Data was analyzed using one-way analysis of variance (ANOVA). Comparisons between different treatment groups were made by Newman-Keuls Multiple Comparison post-test. Results were expressed as the mean +/- standard error of the mean (SEM). A probability of 0.05 of less was deemed statistically significant.

3. RESULTS

3.1. Curcumin Protected RPTEC/TERT1 Against $KBrO_3$ - Induced Cytotoxicity

The potential cytoprotective effect of curcumin was investigated by comparing the activity of the released LDH following the exposure to $KBrO_3$ alone and $KBrO_3$/ curcumin combination. The morphological pattern of cells was assessed using phase contrast microscopy. As shown in Fig. (**1a**), $KBrO_3$ sharply increased the relative activity of LDH at 10mM $KBrO_3$ concentration. The combination of $KBrO_3$ with curcumin exhibited an extremely significant ($p< 0.001$) lowering of LDH release compared to $KBrO_3$ treatment only. These findings revealed that curcumin exhibited a cytoprotective potential against $KBrO_3$ induced cell death

The effect of each treatment on cellular morphology was assessed using phase contrast microscopy (Fig. **1b**). When RPTEC/TERT1 cells were treated with DMSO (i) or with curcumin (ii), the cells showed normal cobblestone appearance, tight interconnections, and formed characteristic domes. Such morphological

characteristics reflect an intact cellular transport system and indicated that the cells were "happy", "healthy", and fully differentiated. Under toxic conditions (iii), $KBrO_3$ caused severe cellular damage with a complete loss of domes and loss of tight junctions between cells. Curcumin clearly minimized $KBrO_3$-induced cellular damage and loss of tight junctions. However, it only partially re-established the characteristic domes of RPTEC/TERT1 cells (Fig. **1b**).

Following 24h exposure, the toxic (IC50) and the subtoxic (IC10) concentrations of $KBrO_3$ were estimated to be 5.5 and 7.5mM, respectively using an LDH release assay (Fig. **1c**).

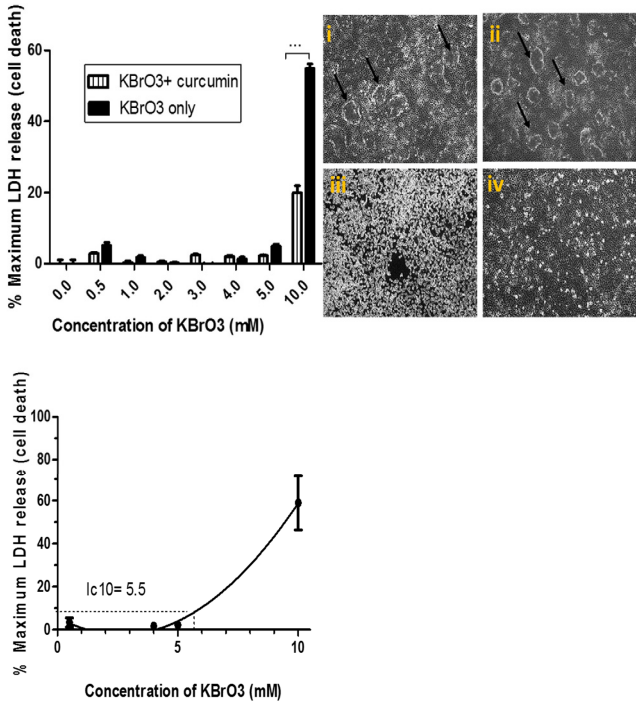

Fig. (1). Examination of the cytoprotective effects of curcumin measured by cytotoxicity assay and assessed by morphological characteristics.

Fig. (1a): The cytoprotective potential of curcumin was assessed using the LDH cytotoxicity assay. RPTEC/TERT1 cells were treated either with the indicated concentrations of $KBrO_3$ only or a combination of $KBrO_3$ concentrations with 25µM curcumin. The figure represents mean± SEM of six independent experiments. (*** = p<0.001)

Fig. (1b): Analysis of the morphological characteristics of RPTEC/TERT1 cells. *C*ells were seeded in 24 well plates, 10 days post 100% confluency, the cells formed fluid filled dooms which reflect a well-functioning transport system. (i) RPTEC/TERT1 were treated with 0.1% DMSO (control), or (ii) with 25µM curcumin for 24h. The domes were maintained and cells were morphologically unaffected by the treatment. (iii) Cells were treated with 10mM $KBrO_3$;. (iv) Cells were treated with the combination of 10mM $KBrO_3$+ 25µM curcumin for 24 hr.

Fig. (1c): Estimation of subtoxic IC10 and the toxic IC50 concentrations of $KBrO_3$. RPTEC/TERT1 cells were seeded in 24 well plates. 10 days post 100% confluency, they were treated with the indicated concentrations of $KBrO_3$ to estimate subtoxic IC10 and the toxic IC50 concentrations. 2% Triton-TX100 was used as a positive control of cell death. The figure represents mean± SEM of six independent experiments.

3.2. Curcumin Suppressed $KBrO_3$ Induced Oxidative Stress and DNA Damage

The potential chemopreventive activity of curcumin was further assessed by comparing the level of oxidative stress following the exposure of RPTEC/TERT1 cells to $KBrO_3$ alone or in combination with curcumin. In this context, intracellular H_2O_2 and 8-OHdG concentrations were measured. Of note, at both IC10 and IC50 concentrations, $KBrO_3$ significantly increased the level of H_2O_2 (p<0.05) (Fig. **2a, b**), and 8-OHdG (p< 0.001) (Fig. **2c, d**) compared to the control or curcumin-only treatment. The combination of curcumin with IC10 or IC50 $KBrO_3$ concentrations significantly (p<0.05) inhibited the levels of both H_2O_2 and 8-OHdG compared to $KBrO_3$ treatment only (Fig. **2a-d***)*. In addition, $KBrO_3$ significantly (p<0.05) reduced catalase gene expression compared to the control or curcumin only treatment. The combination of curcumin with $KBrO_3$, significantly (p<0.05) reversed the negative effect of $KBrO_3$ by upregulating catalase gene expression (Fig. **2e**).

3.3. $KBrO_3$ Induced Dysregulation of Target Genes

The effects of $KBrO_3$ on a panel of 192 genes, was assessed using SYBR green based PCR array technology. These genes are involved in the regulation of inflammation, oxidative stress, angiogenesis, epithelial-mesenchymal transition (EMT), ciliary formation, and apoptosis (supplementary Table **1**).

Following the exposure of RPTEC/TERT1 cells to 5.5mM $KBrO_3$, many genes were dysregulated, as shown in Table **1**. Namely, connective tissue growth factor (CTGF) was the first most overexpressed gene, while interleukin (IL)1-receptor 1 (IL-1R1) was the first most downregulated compared to the untreated RPTEC/TERT1 cells. Genes that were differentially dysregulated in renal cancerous ACHN cells compared to normal RPTEC/TERT1 cells are shown in Table **2**. In this regard, CTGF was one of the top three most overexpressed genes, while IL-1R1 was the most down-regulated gene. The status of genes, that were up-/down-regulated following the exposure of RPTEC/TERT1 cells to $KBrO_3$, was compared to the congruent genes in ACHN cells. ACHN cell line was used as a positive control of carcinogenesis.

Interestingly, we found that a total of 47 genes were differentially dysregulated in the same manner in both $KBrO_3$ treated RPTEC/TERT1 and in the cancerous ACHN cell lines (Table **3**).

3.4. Curcumin Effectively Reduced $KBrO_3$ Induced TRAF3 and IL1-R1 Downregulation and CTGF Upregulation

To validate the results of the PCR array, individual TaqMan-based probe assays were used to measure the expression of TRAF3, IL1-R1, and CTGF quantitatively using qRT-PCR. The exposure of RPTEC/TERT1 to 5.5mM $KBrO_3$ significantly (p<0.001) inhibited TRAF3 and IL-1R1 gene expression compared to untreated or curcumin-treated cells (Fig. **3a** and **3b**). In contrast, $KBrO_3$ treatment significantly (p<0.01) upregulated CTGF gene expression in $KBrO_3$-treated RPTEC/TERT1 compared with untreated or curcumin-treated cells (Fig. **3c**). More importantly, the co-treatment of 25µM curcumin with $KBrO_3$ significantly (p<0.05) diminished the negative effect of $KBrO_3$ on TRAF3 expression (Fig. **3a**), and induced a significant (p<0.01) reduction of the overexpressed CTGF level when combined with $KBrO_3$ compared with $KBrO_3$ alone (Fig. **3c**). However, the protective effect of curcumin on $KBrO_3$ induced IL-1R1 suppression wasn't significant (p>0.05), (Fig. **3b**).

For further validation, we investigated the expression of CTGF at the protein level. In this case, we compared the CTGF repressor activity of curcumin with silymarin, a natural CTGF repressor [27, 28]. $KBrO_3$ clearly up-regulated CTGF protein expression, which was markedly repressed by curcumin. Strikingly, curcumin showed a higher CTGF repressor activity than silymarin when combined with $KBrO_3$ compared with $KBrO_3$-only treatment (Fig. **3d**).

3.5. Curcumin Diminishes the Deciliating Effects of the Genotoxic Carcinogen $KBrO_3$

It has been reported that some renal carcinogens including $KBrO_3$ induce ciliary loss [23]. For this reason, we investigated whether curcumin has a protective potential against $KBrO_3$-induced

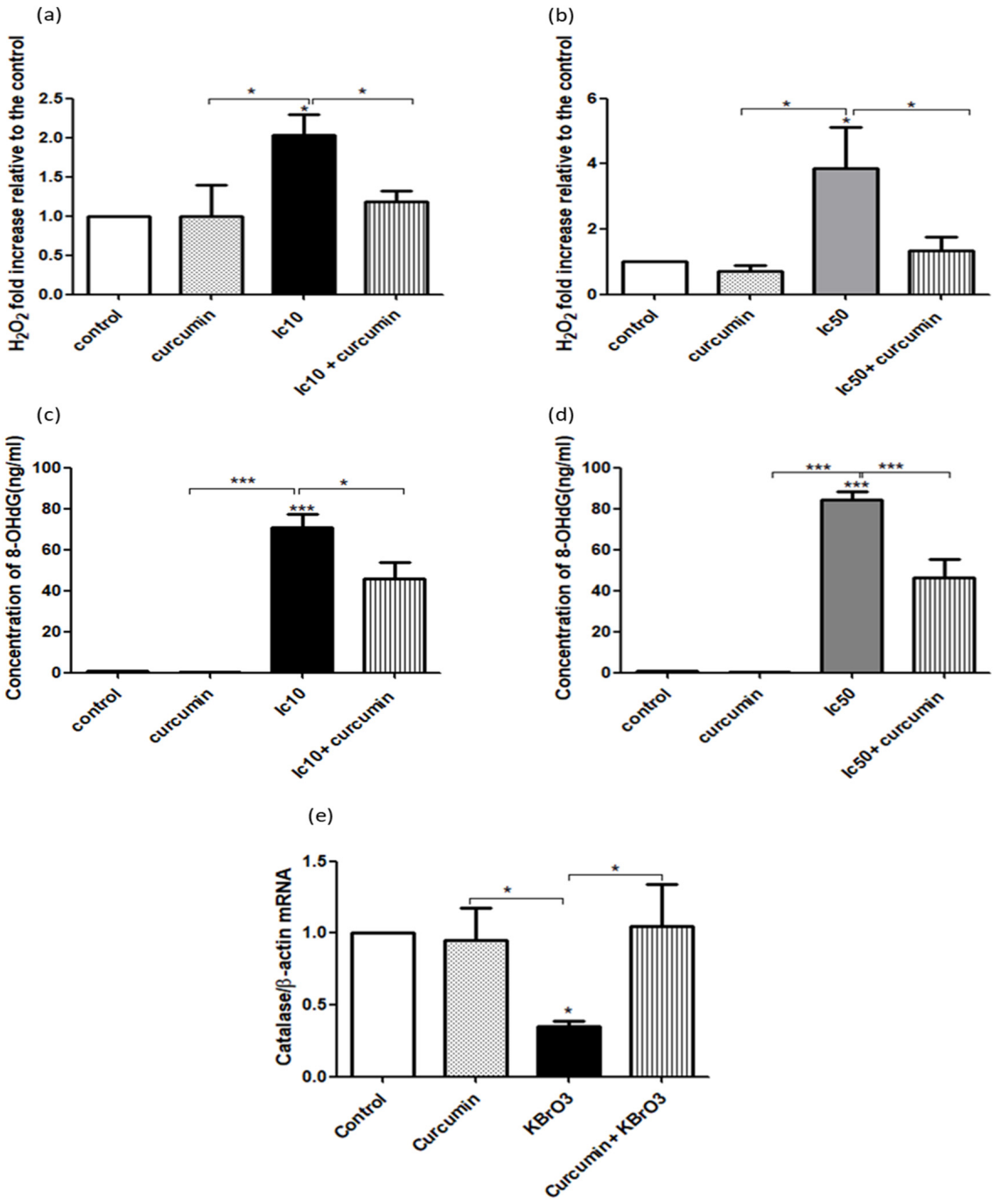

Fig. (2). Analysis of curcumin protection on RPTEC/TERT1 against $KBrO_3$ induced oxidative stress and DNA adduct formation.

Fig. (2a, b) Cells were seeded in 24 well plates until fully confluent. After 10 days, cells were treated with 0.1% DMSO (control), curcumin, $KBrO_3$ and a combination of $KBrO_3$ + curcumin. Intracellular concentration of H_2O_2 was detected using the *Amplex Red* Hydrogen Peroxide Assay Kit. The data represents three independent experiments, *= $p< 0.05$.

Fig. (2c, d) DNA adduct formation was investigated by measuring the intracellular concentration of the DNA adduct 8-OHdG, using the Highly Sensitive 8-OHdG Check ELISA kit following the manufacturer kit instructions. The data represents three independent experiments. *= $p< 0.05$, **= $p<0.01$, and ***=$p <0.001$.

Fig. (2e) Catalase gene expression was examined in $KBrO_3$ (5.5mM) treated RPTEC/TERT1 cells after 24h treatment by RT-PCR analysis (* = $P < 0.05$).

Table 1. List of genes dysregulated following the exposure of RPTEC/TERT1 to $KBrO_3$ for 24h compared with untreated RPTEC/TERT1 cells.

Genes with Markedly Decreased Expression			Genes with Markedly Increased Expression		
Fold Decrease	**Gene Name**	**Gene**	**Fold Increase**	**Gene Name**	**Gene**
-57.7	Interleukin (IL)1-receptor 1	IL1R1	197.55	Connective tissue growth factor	CTGF
-30.89	Toll-like receptor 3	TLR3	37.53	Plasminogen activator inhibitor-1	PAI1
-26.57	Chemokine (C-X-C Motif) Ligand 1	CXCL1	29.92	Resistin	RETN
-25	Interleukin 8	IL8	28.21	Proto-oncogene c-Fos	FOS
-23.08	Chemokine (C-X-C Motif) Ligand 2	CXCL2	15.40	Pim-3 Proto-Oncogene, Serine/Threonine Kinase	PIM3
-22.29	TNF receptor-associated factor 5	TRAF5	16.24	Suppressor of cytokine signaling 1	SOCS1
-20.26	Signal Transducer and Activator of Transcription 1	STAT1	11.66	Tumor necrosis factor	TNFA
-17.5	TNF receptor-associated factor 3	TRAF3	11.28	Toll-like receptor 4	TLR4
-17.49	Myeloid differentiation primary response	MYD88	9.76	Epidermal growth factor	EGF
-13.3	TNF receptor-associated factor 6	TRAF6	9.13	Lymphotoxin-alpha	LTA
-12.9	Chemokine (C-C motif) ligand 20	CCL20	8.50	Nuclear receptor related 1 protein	NR4A2
-11.75	Interleukin 6	IL6	7.02	Ubiquitin C	UBC
-11.59	Caspase 1, Apoptosis-Related Cysteine Peptidase	CASP1	6.18	Adrenoceptor Beta 2, Surface	ADRB2
-9.95	B-Cell CLL/Lymphoma 3	BCL3	6.55	Interleukin-2 receptor alpha	IL2RA
-8.75	Prostaglandin E Receptor 2	PTGER2	4.42	Sex Determining Region Y)-Box 9	SOX9
-8.73	inhibitor of nuclear factor kappa-B kinase	IKBKB	3.16	Tumor Necrosis Factor Receptor Superfamily, Member 10b	TNFRSF10B
-8.35	C-reactive protein	CRP	3.99	Superoxide dismutase	SOD1
-7.41	Plasminogen Activator	PLAT	3.86	(Early Growth Response 2	EGR2
-6.09	Toll-like receptor 2	TLR2	3.78	C-C chemokine receptor type 10	CCR10
-5.87	Janus Kinase 2	JAK2	3.65	Vascular cell adhesion protein 1	VCAM1
-5.57	Mitogen-Activated Protein Kinase Kinase Kinase 1	MAP3K1	3.63	Endothelin 1	EDN1
-5.55	Intercellular Adhesion Molecule 1	ICAM1	3.54	Jun Proto-Oncogene	JUN
-4.78	Complement Component 5	C5	3.38	26S proteasome non-ATPase regulatory subunit 3	PSMD3
-4.33	Leukotriene B4 Receptor 2	LTB4R2	3.31	Nuclear Receptor Subfamily 4	NR4A1
-4.18	Nuclear factor NF-kappa-B p105	NFKB1	2.91	Insulin-Like Growth Factor Binding Protein 2	IGFBP2
-4.17	Insulin-Like Growth Factor Binding Protein 1	IGFBP1	2.48	Retinoic acid receptor alpha	RARA
-4.09	Phospholipase C, Beta 4	PLCB4	2.46	Transforming growth factor beta	TGFB1
-3.99	Chemokine (C-C Motif) Ligand 2	CCL2			
-3.98	TNF receptor-associated factor 2	TRAF2			
-3.83	Signal Transducer And Activator Of Transcription 3	STAT3			

(Table 1) Contd....

Genes with Markedly Decreased Expression			Genes with Markedly Increased Expression		
Fold Decrease	**Gene Name**	**Gene**	**Fold Increase**	**Gene Name**	**Gene**
-3.7	Colony Stimulating Factor 2 Receptor	CSF2			
-3.54	Tumor Necrosis Factor Receptor Superfamily, Member 1A	TNFRSF1A			
-3.32	CAMP Responsive Element Binding Protein 1	CREB1			
-3.32	Nuclear Factor Of Kappa Light Polypeptide Gene Enhancer In B-Cells 2	NFKB2			
-3.16	Insulin-Like Growth Factor Binding Protein 3	IGFBP3			
-2.95	Epidermal Growth Factor Receptor	EGFR			
-2.84	v-rel avian reticuloendotheliosis viral oncogene homolog	REL			
-2.78	Nuclear factor NF-kappa-B p105 subunit	NFKB1			
-2.77	Transforming Growth Factor, Beta Receptor 1	TGFBR1			
-2.74	nterleukin 1 Receptor Antagonist	IL1RN			
-2.43	tumor protein p53	TP53			
-2.35	Mucosa-associated lymphoid tissue lymphoma translocation protein 1	MALT1			
-2.34	V-Rel Avian Reticuloendotheliosis Viral Oncogene Homolog B	RELB			
-2.09	Mitogen-Activated Protein Kinase 8	MAPK8			

Values are expressed as fold change in gene expression relative to vehicle treated control cells. Positive and negative values indicate up- and down-regulation of gene expression, respectively. A fold difference cut-off point was set at ≥2.5.

Table 2. List of genes that were differentially dysregulated in cancerous ACHN cells compared to untreated RPTEC/TERT1 cells.

Genes with Decreased Expression			Genes with Increased Expression		
Fold Decrease	**Gene Name**	**Gene**	**Fold Increase**	**Gene Name**	**Gene**
-53.30	Interleukin (IL)1-receptor 1	IL1R1	185.52	Vascular cell adhesion molecule 1	VCAM1
-51.65	major histocompatibility complex, class I, A	HLAA	23.24	Chemokine (C-C Motif) Receptor 10	CCR10
-46.38	interleukin (IL)1-receptor 1	IL1RN	20.88	Connective Tissue Growth Factor	CTGF
-41.10	Superoxide dismutase 2	SOD2	18.96	Insulin-Like Growth Factor Binding Protein 2	IGFBP2
-39.13	Nuclear receptor related 1 protein	NR4A2	5.86	Resistin	RETN
-29.53	TNF receptor-associated factor 3	TRAF3	3.99	Matrix Metallopeptidase 2	MMP2
-27.81	tumor necrosis factor a (TNF superfamily, member 2	TNFA	3.53	Adrenoceptor Beta 2, Surface	ADRB2
-24.24	Interleukin 6	IL6	3.09	Signal Transducer And Activator Of Transcription 1	STAT1
-21.16	Interleukin 6 receptor	IL6R	3.08	Phospholipase C, Beta 4	PLCB4
-20.59	TNF receptor-associated factor 5	TRAF5	2.87	Early Growth Response-2	EGR2

(Table 2) Contd....

Genes with Decreased Expression			Genes with Increased Expression		
Fold Decrease	**Gene Name**	**Gene**	**Fold Increase**	**Gene Name**	**Gene**
-18.65	C-reactive protein	CRP	2.08	Plasminogen activator inhibitor-1	PAI1
-17.67	Chemokine (C-X-C Motif) Ligand 1	CXCL1	6.11	(Interleukin 2 Receptor, Alpha	IL2RA
-16.81	Intercellular Adhesion Molecule 1	ICAM1	3.58	TATA Box Binding Protein (TBP)-Associated Factor	TRAF1
-16.79	Janus Kinase 2	JAK2	2.55	Toll-Like Receptor 4	TLR4
-15.28	Insulin-Like Growth Factor Binding Protein 3	IGFBP3			
-14.84	Colony Stimulating Factor 2 Receptor, Alpha	CSF2			
-13.78	Transcription factor SOX-9	SOX9			
-13.60	Interleukin-23	IL23			
-12.45	Mitogen-Activated Protein Kinase Kinase Kinase 1	MAP3K1			
-10.66	Colony Stimulating Factor 2 Receptor, Alpha	CSF1			
-9.45	Chemokine (C-X-C Motif) Ligand 2	CXCL2			
-8.77	Transforming Growth Factor, Beta Receptor 1	TGFBR1			
-8.62	Vascular Endothelial Growth Factor A	VEGFA			
-8.50	Prostaglandin E Receptor 2 (Subtype EP2)	PTGER2			
-8.10	Basal Cell Adhesion Molecule	BCAM			
-8.07	Caspase 1, Apoptosis-Related Cysteine Peptidase	CASP1			
-7.80	B-cell lymphoma 6 protein	BCL6			
-7.22	liases for IKBKB Gene	IKBKB			
-6.30	Tumor Necrosis Factor Receptor Superfa-mily, Member 10	TNFRSF10A			
-6.07	Inhibitor Of Kappa Light Polypeptide Gene Enhancer In B-Cells	SCOS3			

Values are expressed as fold change in gene expression relative to vehicle treated control cells. Positive and negative values indicate up- and down-regulation of gene expression, respectively. A fold difference cut-off point was set at ≥2.5.

deciliation. As shown in Fig. (**4a**) *(i) and (ii)*, RPTEC/TERT1 cells were treated with 0.1% DMSO (control) or with 25μM curcumin. Under both conditions, RPTEC/TERT1 exhibited well-defined tight junctional barriers between cells (green), and prominent cilia (red). Treating cells with 5.5mM $KBrO_3$ (iii) resulted in disruption of the tight junctional protein ZO-1 and a complete loss of the ciliary marker protein, acetylated α-tubulin. The co-treatment of curcumin with $KBrO_3$ (iv) minimized ciliary loss and junctional protein damage.

To confirm the results, we investigated the effect of $KBrO_3$ on Arl13b, a specific ciliary protein, using confocal microscopy. Very prominent and intact cilia were observed in both untreated and curcumin-treated cells, as shown in Fig. (**4b**) *(i) and (ii*), respectively. The exposure of RPTEC/TERT1 cells to 5.5mM $KBrO_3$ for 24h caused a significant loss of cilia. In contrast, the co-treatment of 25μM curcumin with $KBrO_3$ clearly reduced the deciliating effect of $KBrO_3$ on RPTEC/TERT1 cells (Fig. **4b** iv).

We also examined gene expression levels of ZO-1 and Arl13b using TaqMan probe-based gene assays, Fig. **4c** and **4d**. As seen in both figures, $KBrO_3$ at 5.5 mM significantly down-regulated the expression of both ZO-1 ($p<0.05$) and Arl13b ($p<0.01$) compared with untreated or curcumin-treated cells. However, the co-treatment of 25μM curcumin with $KBrO_3$ significantly ($p<0.01$) reversed the negative effect of $KBrO_3$ on ZO-1 and Arl13b gene expression.

Table 3. Summary of genes that were dysregulated in both carcinogen ($KBrO_3$) treated RPTEC/TERT1 and in cancerous ACHN cells compared to the untreated RPTEC/TERT1 cells.

Downregulated	Upregulated
BCL3	CTGF
CASP1	PAI1
CCL2	VCAM1
CCL20	RETN
CREB1	CCR10
CRP	IGFBP2
CSF2	ADRB2
CXCL1	EGR2
CXCL2	PAI1
ICAM1	IL2RA
IGFBP1	
IGFBP3	
IKBKB	
IL1R1	
IL1RN	
IL6	
IL8	
JAK2	
LTB4R2	
MAP3K1	
MYD88	
NFKB1	
NFKB1	
NFKB2	
PTGER2	
REL	
RELB	
STAT3	
TGFBR1	
TLR2	
TLR3	
TNFRSF1A	
TP53	
TRAF2	
TRAF3	
TRAF5	
TRAF6	

4. DISCUSSION

Potassium bromate, $KBrO_3$, a salt of the bromate ion, is a nephrotoxic and neurotoxic agent in humans and a proven carcinogen in animals [29, 30]. $KBrO_3$ is considered a possible human carcinogen (IIb) according to the International Agency for Research on Cancer (IARC) [31]. It was used as a model of cancers in many *in vivo* studies [4, 32-34].

The cytotoxic effects of $KBrO_3$ were previously assessed by measuring the activity of the LDH enzyme. Akanji *et al*. found that after administration of a single dose of $KBrO_3$, LDH activity was significantly increased in rat renal and intestinal tissues compared to other tissues [35]. In addition, Ahmed *et al*. reported that the release of LDH from $KBrO_3$- treated cells was linked to $KBrO_3$-induced oxidative stress [36]. In our model, we found that the co-treatment of $KBrO_3$ with curcumin resulted in decreased LDH release which reflects the protective potential of curcumin against $KBrO_3$-induced cytotoxicity. Curcumin has antioxidant, anti-inflammatory, and free radical scavenging activity. Its structure provides two methoxyphenyl groups and an enol form of β-diketone which illicit typical radical trapping activity [37].

In this study, treating human renal RPTEC/TERT1 cells with IC10 or IC50 concentrations of $KBrO_3$ caused an increase of H_2O_2 and 8-OHdG levels suggesting that the induction of oxidative stress is one of the mechanisms by which $KBrO_3$ induces its toxic and carcinogenic effects. We measured H_2O_2 levels as it is more stable than other oxidative species; also, H_2O_2 represents the precursor molecule of the hydroxyl radical that directly targets DNA and forms DNA adducts [38]. The co-treatment of $KBrO_3$ with curcumin suppressed $KBrO_3$ induced elevation of H_2O_2 and 8-OHdG levels at both toxic and subtoxic concentrations. Our findings are in line with a number of previous studies [39-42]. 8-OHdG is a biomarker for oxidative stress and carcinogenicity [43, 44] and has been proven to be a factor in initiating and promoting the process of carcinogenesis [45]. It has been reported that reactive species such as Reactive Oxygen Species (ROS) can attack nucleotide pools such as dGTP forming 8-OHdG. The adduct formed can bind adenine and cytosine nucleotide bases causing A:G mismatch. If the mismatch is irreparable, G:C to A:T transversion, a mutation will form. This mutation is mainly detected in many proto-oncogenes and tumor suppressor genes. In addition, the formation of DNA adducts such as 8-OHdG can cause steric hindrance which affect the fidelity of DNA replication [46]. 8-OHdG is considered as an important biomarker to measure the extent of DNA damage following the exposure to cancer initiating agents. Furthermore, it is also considered as a cofactor of cancer initiation and promotion [47].

Curcumin's chemopreventive potential has been proven by many *in vitro* and *in vivo* studies. Much research has shown that curcumin can efficiently protect cells from H_2O_2 -induced oxidative cell injury [38, 48]. Due to its antioxidant potential, curcumin was shown to have the ability to reduce lipid peroxidation and DNA damage, while increasing the level of vitamin C, vitamin E, and total anti-oxidant capacity [49, 50]. Furthermore, curcumin has been shown to induce phase II metabolism while suppressing phase I metabolizing enzymes such as renal ornithine decarboxylase [51]. Because the catalase enzyme potentially detoxifies and decomposes H_2O_2 to H_2O [52], the activation of catalase by curcumin is considered another effective way to counteract oxidative stress. In this

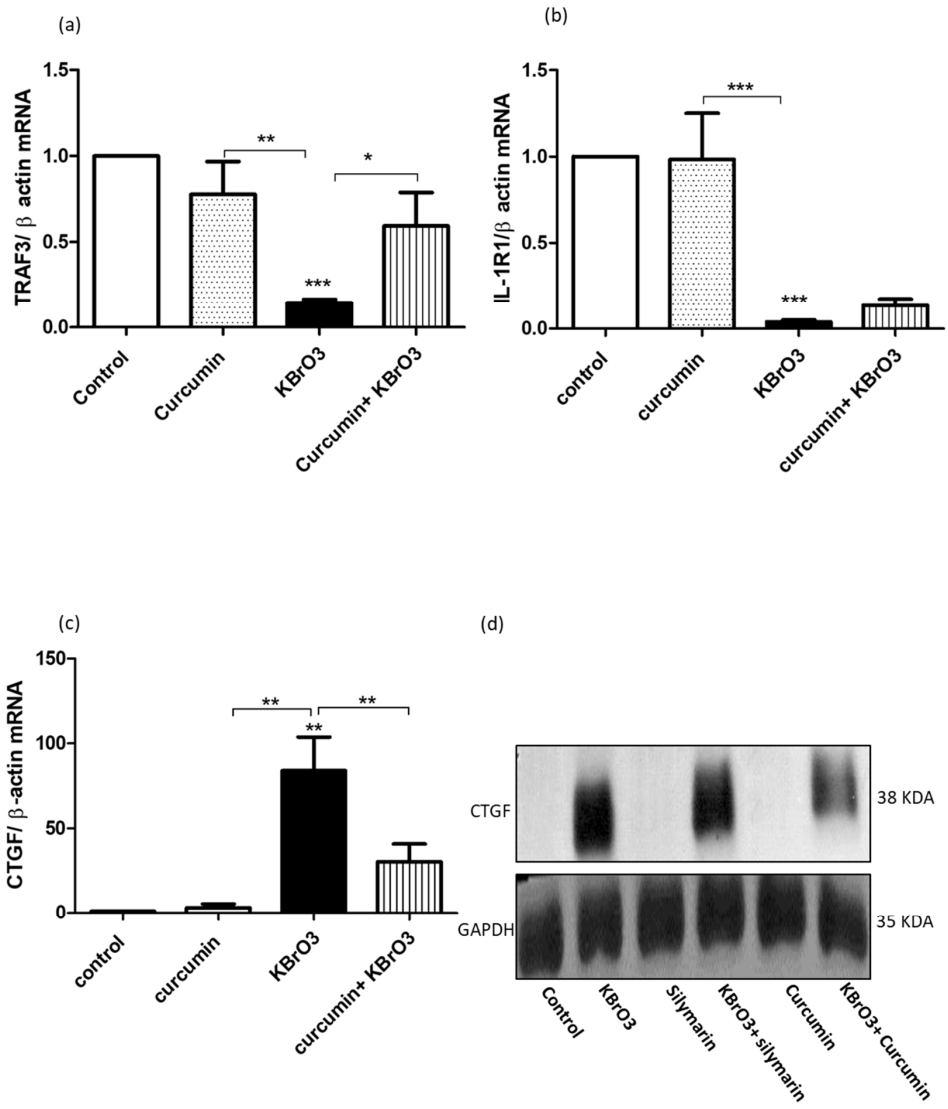

Fig. (3). Analysis of the effects of $KBrO_3$ on TRAF3, IL-1R1, and CTGF gene expression, and the protective potential of curcumin.

Fig. (3a, b) $KBrO_3$ (5.5mM) treatment of RPTEC/TERT1 for 24h onTRAF3 and IL-1 gene expression, respectively compared with the untreated or curcumin-treated cells. Tthe data represents three independent experiments. (*= P> 0.05).

Fig. (3c, d) $KBrO_3$ (5.5mM)- treatment of RPTEC/TERT1 for 24h on CTGF at both mRNA and protein levels in comparison the untreated or curcumin-treated cells. The data represents three independent experiments (**=P < 0.01).

study, $KBrO_3$ was shown to suppress the anti-oxidant catalase enzyme which represents one mechanism by which $KBrO_3$ increases oxidative stress in cells. Our finding is in agreement with a previous study [53]. Interestingly, curcumin effectively reversed $KBrO_3$ induced catalase suppression, which suggests that this may be an important mechanism by which curcumin mediates its chemopreventive effects. Taken together, we can conclude that curcumin blocked the carcinogenic potential of $KBrO_3$ by increasing catalase enzyme activity thus reducing H_2O_2 and 8-OHdG levels.

Previous studies have shown that oxidative DNA damage causes activation of many inflammatory genes which creates a positive feedback loop leading to increased DNA damage, thus promoting cellular transformation and tumor progression [54-56]. Therefore to determine the role of inflammatory genes in our model, we measured a total of 192 target genes following the treatment of RPTEC/TERT1 cells with a subtoxic concentration of $KBrO_3$ and compared the dysregulation status of the genes with the congruent genes in a human renal cancerous ACHN cell line. We found that CTGF was the most overexpressed gene following $KBrO_3$ treatment and the third most overexpressed gene in the cancerous ACHN cell line. To our knowledge, this is the first study to provide evidence of the increased expression of CTGF following $KBrO_3$ treatment at both transcriptional and translational levels. There is abundant evidence from previous studies showing that CTGF can be overexpressed by oxidative stress conditions [57-60], and it has also been shown that CTGF is up-regulated in many cancers [61-64] including renal cell carcinomas [65]. Taken together, we propose that the carcinogenic potential of $KBrO_3$ might be through DNA adduct formation and the dysregulation of several inflammatory-regulating genes including CTGF. We also compared the potential CTGF repressor activity of curcumin with silymarin, another chemopreventive agent with a well-known CTGF repressor activity [27, 66-68]. Co-treatment of curcumin with $KBrO_3$ significantly reduced the expression of CTGF at both RNA and protein levels. Our results are consistent with Zheng and Chen who found that curcumin reduced CTGF overexpression by interfering with upstream TGF-β

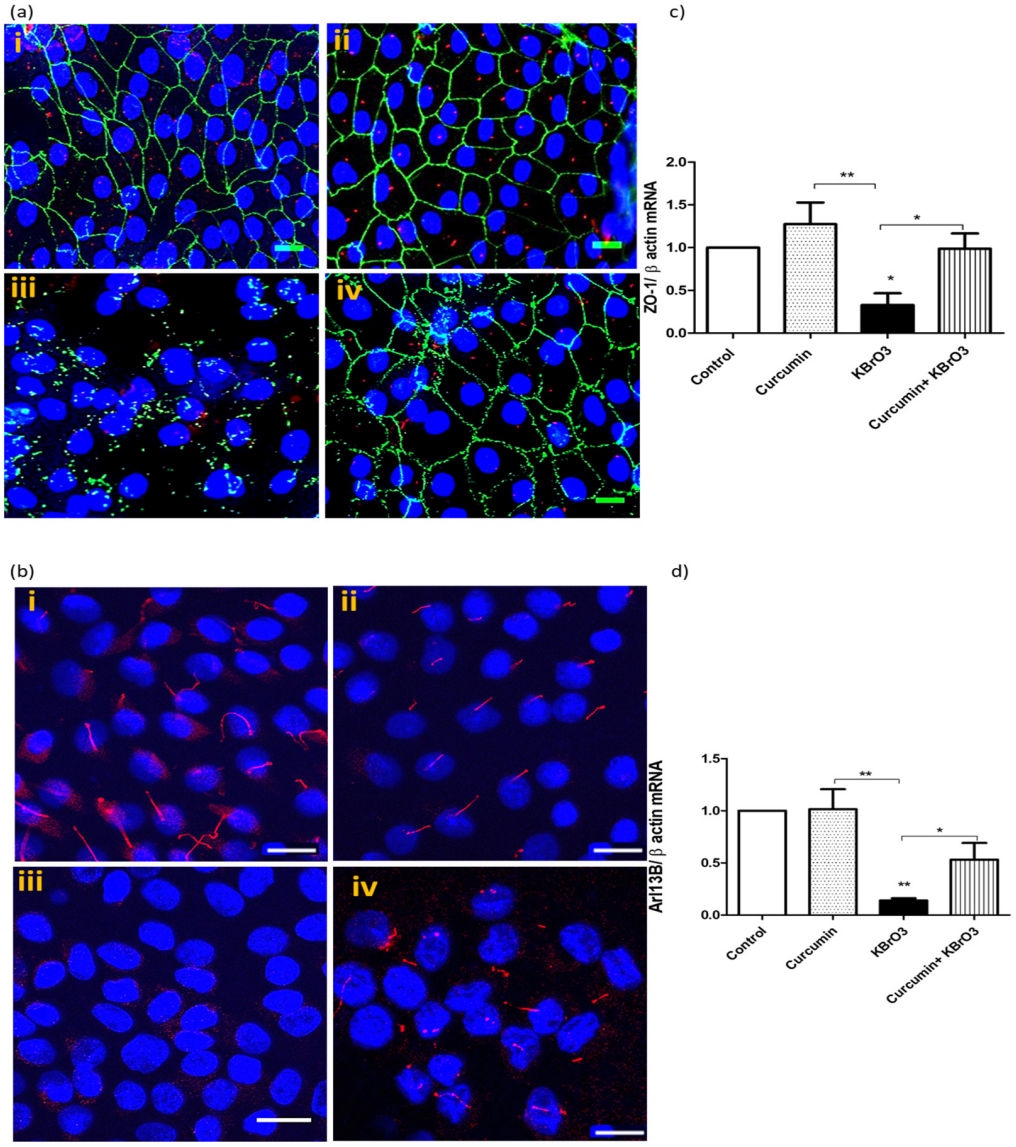

Fig. (4). Effect of Curcumin on $KBrO_3$ induced loss of primary cilia and disruption of tight junction proteins.

Fig. (4a) $KBrO_3$ (5.5mM) treatment of RPTEC/TERT1 for 24h on ciliary and junctional proteins in comparison with untreated or curcumin-treated cells. RPTEC/TERT1 cells were cultured in 8-well chamber slides and treated with after 10 days of 100% confluency. Confocal images (40x) show the primary cilia with red labelled , α-acetylated tubulin, while the green staining represents the tight junctional protein ZO-1. Hoechst 33342 was used to stain the nuclei (blue), scale 50µm. (i) 0.1% DMSO (control), (ii) curcumin 25 µM, (iii) 5.5 mM $KBrO_3$ (ic10) , (iv) Co-treatment of curcumin + $KBrO_3$. The images are representative of 3 independent experiments. Scale =50 µm.

Fig. (4b) $KBrO_3$ (5.5mM) treatment of RPTEC/TERT1 for 24h on a ciliary protein in comparison with untreated or curcumin-treated cells. Confocal images (40x) show the primary cilia with red labelled Arl13b. Hoechst 33342 was used to stain the nuclei (blue), scale 50µm. (i) 0.1% DMSO (control), (ii) curcumin 25 µM, (iii) 5.5 mM $KBrO_3$ (ic10) , (iv) Co-treatment of curcumin + $KBrO_3$. The images are representative of 3 independent experiments.

Fig. (4c, d) $KBrO_3$ (5.5mM) treatment of RPTEC/TERT1 for 24h on ZO-1 and Arl13b gene expression, respectively compared with the untreated or curcumin-treated cells. The data represents three independent experiments. *= p> 0.05, ** = p>0.01. (The color version of the figure is available in the electronic copy of the article).

signaling and TGF-β receptor activation. In addition to this, curcumin was found to induce GSH antioxidant synthesis and peroxisome proliferator-activated receptor (PPAR)-γ activation. Furthermore, curcumin was shown to modulate extracellular matrix gene expression such as α1(I)-collagen fibronectin and α-smooth muscle actin (α-SMA) by interrupting TGF-β signaling including its downstream effector, CTGF [69]. Curcumin halted the CTGF pathway via inhibition of ERK, P38 MAPK, and NF-KB pathways [70-72].

We have also shown that treating human renal RPTEC/TERT1 cells with $KBrO_3$ negatively affected ciliary and junctional protein expression. $KBrO_3$ caused a reduction in the number of ciliated cells and disturbed cellular borders. Our group has previously reported that $KBrO_3$ induced RPTEC/TERT1 ciliary loss was accompanied by an increased proportion of cells at G2/S phase, and thus caused activation of cell cycle progression and proliferation [23]. We have found that curcumin protected RPTEC/TERT1 cells against $KBrO_3$ induced deciliation. Another study showed that curcumin exerted an anti-proliferative effect *via* inhibition of cell cycle regulators of hepatic cells when they were exposed to diethylnitrosamine, a genotoxic carcinogen [73]. Blackmore *et al.* found that curcumin targeted colorectal cancer cells by arresting the G2/M

phase of the cell cycle through disruption of microtubular orientation and assembly, as well as chromosomal condensation and congression [74]. Taken together, these studies show that $KBrO_3$'s deciliating effect caused loss of cellular differentiation and promoted cellular proliferation. Strikingly, such negative effects of $KBrO_3$ were found to be significantly minimized by co-treatment with curcumin in our system.

We have also shown that treating cells with a subtoxic concentration of $KBrO_3$ caused inhibition of IL-1 and TRAF3 gene expression. However the impact of $KBrO_3$ was reduced when treated in combination with curcumin. Il-1 and TRAF3 were selected for further analysis due to their direct link with apoptosis-mediated cell death [75, 76]. Furthermore, it has been found that IL-1 can regulate ciliary length. For instance, a study by Wann and Knight showed that ciliary length increased by approximately 50% following only 3 hours of exposure to IL-1. The mechanism of ciliary elongation is through a protein kinase A (PKA) dependent mechanism [77]. Therefore, by inhibiting IL-1 gene expression, $KBrO_3$ can counteract apoptosis and induce cellular dedifferentiation. TRAF3 is a cytoplasmic component with E3 ubiquitin ligase activity; following the binding to CD40, TRAF3 activates B-lymphocyte cells. It has been found that mice homozygous for a null allele of TRAF3 develop B-cell lymphoma. It also participates in the inhibition of NF-KB signaling pathway, namely interacting with Act 1 in cancer cells. Cells with mutant TRAF3 become cancerous due to the activation of NF-KB [78]. Generally, TRAF3 controls an alternative pathway of NF-KB activation with no effects on the classical pathway. TRAF3 negatively regulates NF-κB inducing kinase (NIK) levels, therefore the mutation of TRAF3 genes or activation of receptor-mediated proteasomal degradation is associated with the accumulation and auto-phosphorylation of NIK and activation of IKKα, which leads to the activation of NF-κB [79]. TRAF3 is sequestered to the cell cytoskeleton via TRAF3 interacting protein 1 (TRAF3ip1) which is localized to the cilium and is necessary for ciliogenesis. TRAF3ip1 mutant cells have been shown to be incapable of generating a primary cilium [80].

We have shown that $KBrO_3$ induced downregulation of NF-KB gene expression at the mRNA level. However, no rescue effect was observed of curcumin against $KBrO_3$-induced NF-KB downregulation (supplementary, Fig. **1**).

A study by Wann *et al.* suggested that primary cilia are considered an important influence on NF-KB activation, thus loss of cilia was associated with deregulation of NF-KB activation [81]. Furthermore, Sinha *et al.* found that TRAF3 can participate in NF-KB activation through the x-linked ectodermal dysplasia receptor [82]. Therefore downregulation of TRAF3, NF-KB, and IL-1 gene expression and disruption of cilia by $KBrO_3$ might be important mechanisms by which to counteract apoptosis and induce cellular dedifferentiation in carcinogenesis. However, further studies are required to investigate the effect of ciliary loss on the expression of inflammatory genes.

A significant number of publications have described curcumin's anti-inflammatory potential as an important property to curtail the progression of several diseases including cancers. Curcumin shows potent anti-inflammatory potential due to its direct regulatory effects on several transcription factors such as STAT, MAPK, and NF-KB, interleukins (ILs) such as TNF-a, IL-1,2,6,8 and 12. Furthermore, it has shown to inhibit lipoxygenase, cyclooxygenase-2 (COX-2), and inducible nitric oxide synthase (iNOS) enzymes activities [83-85].

Despite the broad spectrum of curcumin's health benefits and the wide range of biological significance, its clinical applications are potentially limited due to poor bioavailability. The slight aqueous solubility, instability, and photo degradation of curcumin represent major obstacles that limit its use in different therapeutic applications. Therefore, more than 1500 papers had been published by 2015 to find suitable solutions for such fundamental dilemmas in the clinical use of curcumin [86]. Perhaps, the incorporation of curcumin in a phospholipid system to form a liposomal-curcumin complex is one of the successful trials to improve curcumin's bioavailability. Conjugation of liposomal curcumin with different molecules such as polyethylene glycol and folic acid has been reported to highly extend the biological half-life and targetability of the liposomal curcumin. Therefore, a substantial improvement of both pharmacokinetics and pharmacodynamics of curcumin molecules was recorded following the administration of liposomal curcumin *in vivo* [87]. Other strategies include induction of structural modifications to improve curcumin;s *in vivo* stability and effectiveness. For instance, a recent study has shown that dimethoxy curcumin has a unique anti-tumor activity due to its ability to suppress the transcription factor activator protein-1 (AP-1) and induce degradation of androgen receptors (AR). At the same time, dimethoxy curcumin showed a high metabolic stability compared to curcumin itself [88]. While another study found that a modification in curcumin's aromatic ring resulted in the formation of 10 different curcumin analogues with more potent *in vitro* and *in vivo* anti-tumor activities than curcumin [89]. In this study we provide significant evidence that the food additive $KBrO_3$ induced carcinogenic alteration *via* induction of ROS and activation of several oncogenic genes, counteracting tumor suppressor genes and favouring cell dedifferentiation. To our knowledge, this is the first study to identify the dysregulated genes of $KBrO_3$-treated normal kidney cells that might be implicated in $KBrO_3$-induced carcinogenesis via compar them with the genes of renal cancerous cells. Furthermore, this is the first study to report another protective mechanism of curcumin via inhibition of $KBrO_3$-induced cell dedifferentiation.

CONCLUSION

In conclusion, the molecular mechanisms of curcumin chemoprevention have been investigated and are due in particular to its potential to block $KBrO_3$ induced intracellular oxidative stress, DNA damage, and the dysregulation of signaling hubs that control inflammation, apoptosis, and cell differentiation which contribute to the pathogenesis and progression of $KBrO_3$-induced renal cancer. Although challenges such as poor absorption and rapid elimination represent the major roadblocks in curcumin's clinical applications, research is still ongoing to tackle these problems. However, the future seems bright particularly with the development of new curcumin analogues that are more potent, with higher bioavailability. Therefore, curcumin has considerable scope as a novel cancer prevention agent, due to its pleiotropic actions and in particular its cyto-protective and chemopreventive potential against chemical carcinogenesis.

ETHICS APPROVAL AND CONSENT TO PARTICIPATE

Not applicable.

HUMAN AND ANIMAL RIGHTS

No Animals/Humans were used for studies that are base of this research.

CONSENT FOR PUBLICATION

Not applicable.

CONFLICT OF INTEREST

The authors declare no conflict of interest, financial or otherwise.

ACKNOWLEDGEMENTS

We are grateful to the Iraqi government (MHESR) for fully funding this study, and providing the financial support to undertake all experiments, and to Science Foundation Ireland for funding the UCD Centre for Toxicology, where this project was undertaken.

Appendix

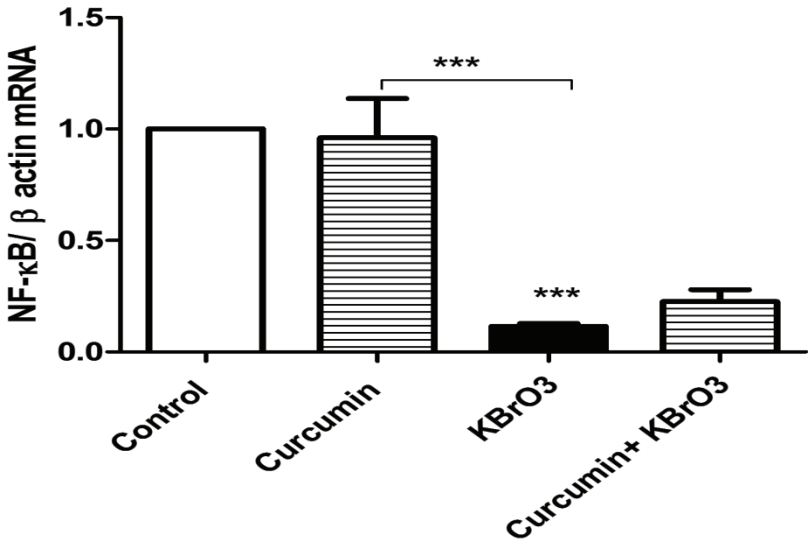

Fig. (S1). Effect of $KBrO_3$ on NF-KB gene expression.
Exposing RPTEC/TERT1 to5.5mM $KBrO_3$ for 24h caused a significant downregulation of NF-KB gene expression compared with control. The combination of curcumin with $KBrO_3$ slightly but non-significantly reversed the negative effect of $KBrO_3$ on NF-KB gene expression. The data represents three independent experiments.

Table S1. Symbols and names of 187 inflammation-associated genes screened in gene expression array.

Gene Symbols	Gene Name
ACTB	Beta actin
ADRB2	ADRB2 adrenoceptor beta 2(ADRB2) *Homo sapiens*
AKT1	v-akt murine thymoma viral oncogene homolog 1
BCAM	BCAM basal cell adhesion molecule
BCL3	BCL3 B-cell CLL/lymphoma 3(BCL3) *Homo sapiens*
BCL6	BCL6 B-cell CLL/lymphoma 6(BCL6) *Homo sapiens*
BCMA	B-Cell Maturation Protein
C3	Complement component 3
C5	C5 complement C5(C5) *Homo sapiens*
CASP1	CASP1 caspase 1(CASP1) *Homo sapiens*
CCL11	CCL11 C-C motif chemokine ligand 11(CCL11) *Homo sapiens*
CCL13	CCL13 C-C motif chemokine ligand 13(CCL13) *Homo sapiens*
CCL15	Chemokine (C-C motif) ligand 15
CCL16	Chemokine (C-C motif) ligand 16
CCL17	Chemokine (C-C motif) ligand 17
CCL18	CCL18 C-C motif chemokine ligand 18(CCL18) *Homo sapiens*
CCL19	CCL19 C-C motif chemokine ligand 19(CCL19) *Homo sapiens*
CCL2	CCL2 C-C motif chemokine ligand 2(CCL2) *Homo sapiens*
CCL20	Chemokine (C-C motif) ligand 20

(Table 1) Contd....

Gene Symbols	Gene Name
CCL21	CCL21 C-C motif chemokine ligand 21(CCL21) *Homo sapiens*
CCL22	CCL22 C-C motif chemokine ligand 22(CCL22) *Homo sapiens*
CCL23	CCL23 C-C motif chemokine ligand 23(CCL23) *Homo sapiens*
CCL25	Chemokine (C-C motif) ligand 25
CCL3	CCL3 C-C motif chemokine ligand 3(CCL3) *Homo sapiens*
CCL4	CCL4 C-C motif chemokine ligand 4(CCL4) *Homo sapiens*
CCL5	CCL5 C-C motif chemokine ligand 5(CCL5) *Homo sapiens*
CCL7	CCL7 C-C motif chemokine ligand 7(CCL7) *Homo sapiens*
CCL8	CCL8 C-C motif chemokine ligand 8(CCL8) *Homo sapiens*
CCR1	Chemokine (C-C motif) receptor 1
CCR10	CCR10 C-C motif chemokine receptor 10(CCR10) *Homo sapiens*
CCR2	CCR2 C-C motif chemokine receptor 2(CCR2) *Homo sapiens*
CCR3	CCR3 C-C motif chemokine receptor 3(CCR3) *Homo sapiens*
CCR4	Chemokine (C-C motif) receptor 4
CCR5	Chemokine (C-C motif) receptor 5
CCR6	Chemokine (C-C motif) receptor 6
CCR7	CCR7 C-C motif chemokine receptor 7(CCR7) *Homo sapiens*
CCR8	Chemokine (C-C motif) receptor 8
CCR9	CCR9 C-C motif chemokine receptor 9(CCR9) *Homo sapiens*
CD14	CD14 molecule
CD4	CD4 CD4 molecule(CD4) *Homo sapiens*
CD40	CD40 molecule, TNF receptor superfamily member 5
CD83	CD83 molecule
CD88	Complement C5a receptor 1
CD8A	CD8A CD8a molecule(CD8A) *Homo sapiens*
CD8B	CD8B CD8b molecule(CD8B) *Homo sapiens*
CLEC7A	C-type lectin domain family 7, member A
CREB1	cAMP responsive element binding protein 1
CREB1	CREB1 cAMP responsive element binding protein 1(CREB1)
CRP	C-reactive protein, pentraxin-related
CSF1	CSF1 colony stimulating factor 1(CSF1) *Homo sapiens*
CSF1R	CSF1R colony stimulating factor 1 receptor(CSF1R) *Homo sapiens*
CSF2	CSF2 colony stimulating factor 2(CSF2) *Homo sapiens*
CTGF	CTGF connective tissue growth factor(CTGF) *Homo sapiens*
CXCL1	CXCL1 C-X-C motif chemokine ligand 1(CXCL1) *Homo sapiens*
CXCL13	CXCL13 C-X-C motif chemokine ligand 13(CXCL13) *Homo sapiens*
CXCL2	CXCL2 C-X-C motif chemokine ligand 2(CXCL2) *Homo sapiens*

(Table 1) Contd....

Gene Symbols	Gene Name
CXCL3	CXCL3 C-X-C motif chemokine ligand 3(CXCL3) *Homo sapiens*
CXCL5	CXCL5 C-X-C motif chemokine ligand 5(CXCL5) *Homo sapiens*
CYSLTR1	Cysteinyl leukotriene receptor 1
EDN1	EDN1 endothelin 1(EDN1) *Homo sapiens*
EGF	EGF epidermal growth factor(EGF) *Homo sapiens*
EGFR	EGFR epidermal growth factor receptor(EGFR) *Homo sapiens*
EGR2	EGR2 early growth response 2(EGR2) *Homo sapiens*
F2	F2 coagulation factor II, thrombin(F2) *Homo sapiens*
FOS	FOS Fos proto-oncogene, AP-1 transcription factor subunit
GAPDH	Glyceraldehyde-3-phosphate dehydrogenase
GSTP1	GSTP1 glutathione S-transferase pi 1(GSTP1) *Homo sapiens*
GUSB	Glucuronidase, beta
HIF1A	HIF1A hypoxia inducible factor 1 alpha subunit(HIF1A) *Homo sapiens*
HLAA	Major histocompatibility complex, class I, A
HLAB	Major histocompatibility complex, class I, B [*Homo sapiens*
HPRT1	Hypoxanthine phosphoribosyltransferase 1
HPRT1	HPRT1 hypoxanthine phosphoribosyltransferase 1(HPRT1)
HRH3	Histamine receptor H3
ICAM1	Intercellular adhesion molecule 1
IFNG	Interferon gamma
IGFBP1	IGFBP1 insulin like growth factor binding protein 1(IGFBP1)
IGFBP2	IGFBP2 insulin like growth factor binding protein 2(IGFBP2)
IGFBP3	IGFBP3 insulin like growth factor binding protein 3(IGFBP3)
IKBKB	Inhibitor of kappa light polypeptide gene enhancer in B-cells, kinase beta
IL10	Interleukin 10
IL12B	Interleukin 12b
IL15	IL15 interleukin 15(IL15) *Homo sapiens*
IL17A	Interleukin 17A
IL1B	Interleukin 1, beta
IL1R1	Interleukin 1 receptor, type I
IL1RN	Interleukin 1 receptor antagonist
IL2	Interleukin 2
IL23	Interleukin 23
IL24	Interleukin 24(IL24)
IL2RA	Interleukin 2 receptor, alpha
IL4	Interleukin 4
IL5	Interleukin 5

(Table 1) Contd....

Gene Symbols	Gene Name
IL6	Interleukin 6
IL6R	Interleukin 6 receptor
IL6ST	Interleukin 6 signal transducer
IL8	Interleukin 8
INSR	Insulin receptor
IRAK1	Interleukin 1 receptor associated kinase 1
IRAK2	Interleukin 1 receptor associated kinase 2
IRF1	Interferon regulatory factor 1
JAK2	Janus kinase 2
JUN	Jun proto-oncogene, AP-1 transcription factor subunit(JUN)
LCN2	Lipocalin 2
LTA	Lymphotoxin alpha
LTB4R2	Leukotriene B4 receptor 2
LTC4S	Leukotriene C4 synthase
MALT1	Mucosa associated lymphoid tissue lymphoma translocation gene 1
MAP3K1	Mitogen-activated protein kinase kinase kinase 1
MAPK1	Mitogen-activated protein kinase 1
MAPK8	Mitogen-activated protein kinase 8
MMP1	Matrix metallopeptidase 1 (interstitial collagenase)
MMP13	Matrix metallopeptidase 13 (collagenase 3)
MMP2	MMP2 matrix metallopeptidase 2(MMP2) *Homo sapiens*
MMP3	MMP3 matrix metallopeptidase 3(MMP3) *Homo sapiens*
MMP9	Matrix metallopeptidase 9 (gelatinase B, 92 kDa gelatinase, 92 kDa type IV collagenase)
MTHFR	Methylenetetrahydrofolate reductase (NAD(P)H)
MUC5AC	MUC5AC mucin 5AC, oligomeric mucus/gel-forming(MUC5AC)
MYD88	Myeloid differentiation primary response gene 88
NFKB1	NFKB1 nuclear factor kappa B subunit 1(NFKB1) *Homo sapiens*
NFKB1A	Nuclear factor kappa B 1 A
NFKB2	Nuclear factor of kappa light polypeptide gene enhancer in B-cells 2 (p49/p100)
NOD2	NOD2 nucleotide binding oligomerization domain containing 2(NOD2)
NOS2	Nitric oxide synthase 2, inducible
NR2C2	Nuclear receptor subfamily 2, group C, member 2
NR3C1	Nuclear receptor subfamily 3, group C, member 1 (glucocorticoid receptor)
NR4A1	Nuclear receptor subfamily 4, group A, member 1
NR4A1	Nuclear receptor subfamily 4 group A member 1
NR4A2	Nuclear receptor subfamily 4, group A, member 2
PAI1	Plasminogen activator inhibitor-1

(Table 1) Contd....

Gene Symbols	Gene Name
PCK1	PCK1 phosphoenolpyruvate carboxykinase 1
PIM1	PIM1 Pim-1 proto-oncogene, serine/threonine kinase
PIM2	Pim-2 proto-oncogene, serine/threonine kinase
PIM3	Pim-3 proto-oncogene, serine/threonine kinase
PLA2G2D	Phospholipase A2, group IID
PLAT	Plasminogen activator, tissue type
PLCB4	Phospholipase C beta 4(PLCB4) *Homo sapiens*
PPARG	Peroxisome proliferator-activated receptor gamma
PSMD3	Proteasome 26S subunit, non-ATPase 3
PTGER1	Prostaglandin E receptor 1 (subtype EP1)
PTGER2	Prostaglandin E receptor 2 (subtype EP2)
PTGS2	Prostaglandin-endoperoxide synthase 2
RARA	Retinoic acid receptor alpha
REL	v-rel avian reticuloendotheliosis viral oncogene homolog
RELA	v-rel avian reticuloendotheliosis viral oncogene homolog A
RELB	RELB proto-oncogene, NF-kB subunit
RELMB	Resistin-Like Molecule-beta
RETN	RETN resistin(RETN) *Homo sapiens*
RIPK1	Receptor (TNFRSF)-interacting serine-threonine kinase 1
SELE	Selectin E
SOCS1	Suppressor of cytokine signaling 1
SOCS3	Suppressor of cytokine signaling 3
SOD1	SOD1 superoxide dismutase 1, soluble(SOD1)
SOD2	SOD2 superoxide dismutase 2, mitochondrial(SOD2)
SOX9	SRY (sex determining region Y)-box 9
STAT1	Signal transducer and activator of transcription 1(STAT1)
STAT3	Signal transducer and activator of transcription 3
TBP	TATA-box binding protein
TGFB1	Transforming growth factor, beta 1
TGFB1	Transforming growth factor beta 1
TGFB2	Transforming growth factor beta 2
TGFBR1	TGFBR1 transforming growth factor beta receptor 1
TIRAP	Toll-interleukin 1 receptor (TIR) domain containing adaptor protein
TIRAP	TIR domain containing adaptor protein
TLR1	Toll-like receptor 1
TLR2	Toll-like receptor 2
TLR3	Toll-like receptor 3

(Table 1) Contd....

Gene Symbols	Gene Name
TLR4	Toll-like receptor 4
TLR6	Toll-like receptor 6
TLR7	Toll-like receptor 7
TLR8	Toll-like receptor 8
TNFA	Tumor necrosis factor a (TNF superfamily, member 2)
TNFRSF10A	TNF receptor superfamily member 10a
TNFRSF10B	Tumor necrosis factor receptor superfamily, member 10b
TNFRSF1A	Tumor necrosis factor receptor superfamily, member 1A
TNFSF18	Tumor necrosis factor (ligand) superfamily, member 18
TP53	Tumor protein p53
TRAF1	TNF receptor-associated factor 1
TRAF2	TNF receptor-associated factor 2
TRAF3	TNF receptor-associated factor 3
TRAF5	TNF receptor-associated factor 5
TRAF6	TNF receptor-associated factor 6
UBC	UBC ubiquitin C(UBC)
VCAM	Vascular cell adhesion molecule
VCAM1	Vascular cell adhesion molecule 1
VEGF	Vascular endothelial growth factor
VEGFA	Vascular endothelial growth factor A

REFERENCES

[1] Radford R, Frain H, Ryan MP, Slattery C, McMorrow T. Mechanisms of chemical carcinogenesis in the kidneys. Int J Mol Sci 2013;14(10):19416-33.

[2] U.S Food & Drug adminstration. Requirements for Specific Standardized Bakery Products [Internet]. 2017. Available from: https://www.accessdata.fda.gov/scripts/cdrh/cfdocs/cfcfr/cfrsearch.cfm?fr=136.110.

[3] Ishidate M, Yoshikawa K. Chromosome Aberration Tests with Chinese Hamster Cells *in vitro* with and without Metabolic Activation — A Comparative Study on Mutagens and Carcinogens. In: Chambers PL, Klinger W, editors. Further Studies in the Assessment of Toxic Actions: Proceedings of the European Society of Toxicology Meeting, Held in Dresden, June 11 – 13, 1979. Berlin, Heidelberg: Springer Berlin Heidelberg; 1980. p. 41-4.

[4] Kasai H, Nishimura S, Kurokawa Y, Hayashi Y. Oral administration of the renal carcinogen, potassium bromate, specifically produces 8-hydroxydeoxyguanosine in rat target organ DNA. Carcinogenesis 1987; 8(12): 1959-61.

[5] DeAngelo AB, George MH, Kilburn SR, Moore TM, Wolf DC. Carcinogenicity of potassium bromate administered in the drinking water to male B6C3F1 mice and F344/N rats. Toxicol Pathol 1998; 26(5): 587-94.

[6] Shiao YH, Kamata SI, Li LM, *et al*. Mutations in the VHL gene from potassium bromate-induced rat clear cell renal tumors. Cancer Lett 2002; 187(1-2): 207-14.

[7] Ballmaier D, Epe B. Oxidative DNA damage induced by potassium bromate under cell-free conditions and in mammalian cells. Carcinogenesis 1995; 16(2): 335-42.

[8] Parsons JL, Chipman JK. The role of glutathione in DNA damage by potassium bromate *in vitro*. Mutagenesis 2000; 15(4): 311-6.

[9] Ballmaier D, Epe B. DNA damage by bromate: Mechanism and consequences. Toxicology 2006; 221(2-3): 166-71.

[10] Bader HL, Hsu T. Systemic VHL gene functions and the VHL disease. Febs Lett 2012; 586(11): 1562-9.

[11] Michaud EJ, Yoder BK. The Primary Cilium in Cell Signaling and Cancer. Cancer Res 2006; 66(13): 6463-7.

[12] Pan J, Seeger-Nukpezah T, Golemis EA. The role of the cilium in normal and abnormal cell cycles: Emphasis on renal cystic pathologies. Cell Mol Life Sci 2013; 70(11): 1849-74.

[13] Quarmby LM, Parker JDK. Cilia and the cell cycle? J. Cell Biol 2005; 169(5): 707-10.

[14] Schraml P, Frew IJ, Thoma CR, *et al*. Sporadic clear cell renal cell carcinoma but not the papillary type is characterized by severely reduced frequency of primary cilia. Mod Pathol 2009; 22(1): 31-6.

[15] Mehta RG, Murillo G, Naithani R, Peng X. Cancer chemoprevention by natural products: how far have we come? Pharm Res 2010; 27(6): 950-61.

[16] Aggarwal BB, Sundaram C, Malani N, Ichikawa H. Curcumin: the Indian solid gold. The molecular targets and therapeutic uses of curcumin in health and disease: Springer; 2007: 1-75.

[17] Steward WP, Brown K. Cancer chemoprevention: a rapidly evolving field. Br J Cancer 2013; 109(1): 1-7.

[18] Chendil D, Ranga RS, Meigooni D, Sathishkumar S, Ahmed MM. Curcumin confers radiosensitizing effect in prostate cancer cell line PC-3. Oncogene 2004; 23(8): 1599-607.

[19] Gupta SC, Patchva S, Koh W, Aggarwal BB. Discovery of curcumin, a component of golden spice, and its miraculous biological activities. Clin Exp Pharmacol Physiol 2012; 39(3): 283-99.

[20] Uzzan B, Benamouzig R. Is Curcumin a Chemopreventive Agent for Colorectal Cancer? Curr Colorectal Cancer Rep 2016; 12(1): 35-41.

[21] Momtazi AA, Shahabipour F, Khatibi S, Johnston TP, Pirro M, Sahebkar A. Curcumin as a MicroRNA Regulator in Cancer: A Review. Rev Physiol Biochem Pharmacol 2016; 171: 1-38.

[22] Banikazemi Z, Haji HA, Mohammadi M, *et al*. Diet and cancer prevention: Dietary compounds, dietary MicroRNAs, and dietary exosomes. J Cell Biochem 2018; 119(1): 185-96.

[23] Radford R, Slattery C, Jennings P, *et al*. Carcinogens induce loss of the primary cilium in human renal proximal tubular epithelial cells independently of effects on the cell cycle. Am J Physiol Renal Physiol 2012; 302(8): F905-16.

[24] Wieser M, Stadler G, Jennings P, *et al*. hTERT alone immortalizes epithelial cells of renal proximal tubules without changing their functional characteristics. Am J Physiol Renal Physiol 2008; 295(5): F1365-75.

[25] Robertson R, Guihéneuf F, Bahar B, *et al*. The Anti-Inflammatory Effect of Algae-Derived Lipid Extracts on Lipopolysaccharide (LPS)-Stimulated Human THP-1 Macrophages. Mar Drugs 2015; 13(8): 5402.

[26] Buchmann K, Pedersen L, Glamann J. Humoral immune response of European eel Anguilla anguilla to a major antigen in Anguillicola crassus (Nematoda). Dis Aquat Organ 1991; 12(1): 55-7.

[27] Tzeng JI, Chen MF, Chung HH, Cheng JT. Silymarin decreases connective tissue growth factor to improve liver fibrosis in rats treated with carbon tetrachloride. Phytother Res 2013; 27(7): 1023-8.

[28] Duval F, Moreno-Cuevas JE, González-Garza MT, Rodríguez-Montalvo C, Cruz-Vega DE. Protective mechanisms of medicinal plants targeting hepatic stellate cell activation and extracellular matrix deposition in liver fibrosis. Chin Med 2014; 9(1): 27.

[29] IARC. IARC monographs on the evaluation of the carcinogenic risk of chemicals to humans; Sorne Naturally Occurring and Synthetic Food Cornponents, Furocournarins and Ultraviolet Radiation. Volume 40, Lyon -France, P 207-220: 1986.

[30] Geter DR, Ward WO, Knapp GW, *et al*. Kidney Toxicogenomics of Chronic Potassium Bromate Exposure in F344 Male Rats. Transl Oncogenomics 2006; 1: 33-52.

[31] IARC. Evaluation of carcinogenic risks to humans. OverаII Evaluations of Carcinogenicity:An Updating of IARC Monographs. Supplement 7, volume 1-42, Lyon, France, page 70 ; 1987.

[32] Kurokawa Y, Takayama S, Konishi Y, *et al*. Long-term *in vivo* carcinogenicity tests of potassium bromate, sodium hypochlorite, and sodium chlorite conducted in Japan. Environ Health Perspect 1986; 69: 221-35.

[33] Kurokawa Y, Aoki S, Matsushima Y, Takamura N, Imazawa T, Hayashi Y. Dose-Response Studies on the Carcinogenicity of Potassium Bromate in F344 Rats After Long-Term Oral Administration. J Natl Cancer Inst 1986; 77(4): 977-82.

[34] Sakamoto K, Tominaga Y, Yamauchi K, *et al*. MUTYH-Null Mice Are Susceptible to Spontaneous and Oxidative Stress–Induced Intestinal Tumorigenesis. Cancer res 2007; 67(14): 6599-604.

[35] Akanji M, Nafiu M, Yakubu M. Enzyme activities and histopathology of selected tissues in rats treated with potassium bromate. Afr J Biomed Res 2008; 11(1).

[36] Ahmad MK, Khan AA, Ali SN, Mahmood R. Chemoprotective effect of taurine on potassium bromate-induced DNA damage, DNA-protein cross-linking and oxidative stress in rat intestine. PLoS One 2015; 10(3): e0119137.

[37] Masuda T, Maekawa T, Hidaka K, Bando H, Takeda Y, Yamaguchi H. Chemical Studies on Antioxidant Mechanism of Curcumin: Analysis of Oxidative Coupling Products from Curcumin and Linoleate. J Agric Food Chem 2001; 49(5): 2539-47.

[38] Mahakunakorn P, Tohda M, Murakami Y, Matsumoto K, Watanabe H, Vajaragupta O. Cytoprotective and cytotoxic effects of curcumin: dual action on H2O2-induced oxidative cell damage in NG108-15 cells. Biol Pharm Bull 2003; 26(5): 725-8.

[39] Kurokawa Y, Maekawa A, Takahashi M, Hayashi Y. Toxicity and carcinogenicity of potassium bromate--a new renal carcinogen. Environ Health Perspect 1990; 87: 309-35.

[40] Giri U, Iqbal M, Athar M. Potassium bromate ($KBrO_3$) induces renal proliferative response and damage by elaborating oxidative stress. Cancer Lett 1999; 135(2): 181-8.

[41] Khan RA, Khan MR, Sahreen S, *et al*. Potassium bromate ($KBrO_3$) induced nephrotoxicity: protective effects of n-hexane extract of Sonchus asper. J Med Plants Res 2011; 5(25): 6017-23.

[42] Khan RA, Khan MR, Sahreen S. Protective effects of rutin against potassium bromate induced nephrotoxicity in rats. BMC Complement Altern Med 2012; 12(1): 204.

[43] Kasai H. Analysis of a form of oxidative DNA damage, 8-hydroxy-2'-deoxyguanosine, as a marker of cellular oxidative stress during carcinogenesis. Mutat Res 1997; 387(3): 147-63.

[44] Nakae D, Umemura T, Kurokawa Y. Reactive oxygen and nitrogen oxide species-induced stress, a major intrinsic factor involved in carcinogenic processes and a possible target for cancer prevention. Asian Pac J Cancer Prev 2002; 3: 313-8.

[45] Valavanidis A, Vlachogianni T, Fiotakis C. 8-hydroxy-2′ -deoxyguanosine (8-OHdG): A Critical Biomarker of Oxidative Stress and Carcinogenesis. J Environ Sci Health C Environ Carcinog Ecotoxicol Rev 2009; 27(2): 120-39.

[46] Klaunig JE, Kamendulis LM, Hocevar BA. Oxidative stress and oxidative damage in carcinogenesis. Toxicol Pathol 2010; 38(1): 96-109.

[47] Valavanidis A, Vlachogianni T Fau - Fiotakis C, Fiotakis C. 8-hydroxy-2' -deoxyguanosine (8-OHdG): A critical biomarker of oxidative stress and carcinogenesis 2009(1532-4095 (Electronic)).

[48] Cohly HHP, Taylor A, Angel MF, Salahudeen AK. Effect of Turmeric, Turmerin and Curcumin on H2O2-Induced Renal Epithelial (LLC-PK1) Cell Injury. Free Radic Biol Med 1998; 24(1): 49-54.

[49] Rai B, Kaur J, Jacobs R, Singh J. Possible action mechanism for curcumin in pre-cancerous lesions based on serum and salivary markers of oxidative stress. J Oral Sci 2010; 52(2): 251-6.

[50] Ciftci G, Aksoy A, Cenesiz S, *et al*. Therapeutic role of curcumin in oxidative DNA damage caused by formaldehyde. Microsc Res Tech 2015; 78(5): 391-5.

[51] Iqbal M, Okazaki Y, Okada S. Curcumin attenuates oxidative damage in animals treated with a renal carcinogen, ferric nitrilotriacetate (Fe-NTA): implications for cancer prevention. Mol Cell Biochem 2009; 324(1): 157-64.

[52] Petrucci RH. General Chemistry: Principles & Modern Applications (9th ed.): Prentice Hall; 2007.

[53] Watanabe S, Tajima Y, Yamaguchi T, Fukui T. Potassium bromate-induced hyperuricemia stimulates acute kidney damage and oxidative stress. J Health Sci 2004; 50(6): 647-53.

[54] Coussens LM, Werb Z. Inflammation and cancer. Nature 2002; 420(6917): 860-7.

[55] Reuter S, Gupta SC, Chaturvedi MM, Aggarwal BB. Oxidative stress, inflammation, and cancer: How are they linked? Free Radic Biol Med 2010; 49(11): 1603-16.

[56] Halliday GM. Inflammation, gene mutation and photoimmunosuppression in response to UVR-induced oxidative damage contributes to photocarcinogenesis. Mutat Res/Fund Mol M 2005; 571(1-2): 107-20.

[57] Ohshiro Y, Ma RC, Yasuda Y, *et al*. Reduction of diabetes-induced oxidative stress, fibrotic cytokine expression, and renal dysfunction in protein kinase Cβ–null mice. Diabetes 2006; 55(11): 3112-20.

[58] Park SK, Kim J, Seomun Y, *et al*. Hydrogen peroxide is a novel inducer of connective tissue growth factor. Biochem Biophys Res Commun 2001; 284(4): 966-71.

[59] Branchetti E, Poggio P, Sainger R, *et al*. Oxidative stress modulates vascular smooth muscle cell phenotype via CTGF in thoracic aortic aneurysm. Cardiovasc Res 2013; 100(2): 316-24.

[60] Matsuda S, Gomi F, Katayama T, Koyama Y, Tohyama M, Tano Y. Induction of connective tissue growth factor in retinal pigment epithelium cells by oxidative stress. Jpn J Ophthalmol 2006; 50(3): 229-34.

[61] Wenger C, Ellenrieder V, Alber B, *et al*. Expression and differential regulation of connective tissue growth factor in pancreatic cancer cells. Oncogene 1999; 18(4): 1073-80.

[62] Jiang WG, Watkins G, Fodstad O, Douglas-Jones A, Mokbel K, Mansel RE. Differential expression of the CCN family members Cyr61, CTGF and Nov in human breast cancer. Endocr-Relat Cancer 2004; 11(4): 781-91.

[63] Chen P-P, Li W-J, Wang Y, *et al*. Expression of Cyr61, CTGF, and WISP-1 correlates with clinical features of lung cancer. PloS one 2007; 2(6): e534.

[64] Chu C-Y, Chang C-C, Prakash E, Kuo M-L. Connective tissue growth factor (CTGF) and cancer progression. J Biomed Sci 2008; 15(6): 675-85.

[65] Chintalapudi MR, Markiewicz M, Kose N, *et al*. Cyr61/CCN1 and CTGF/CCN2 mediate the proangiogenic activity of VHL-mutant renal carcinoma cells. Carcinogenesis 2008; 29(4): 696-703.

[66] ZHAO Y-z, XIAO X-h, QI Z-p, LIU Z, BO X-t. Effect of silymarin on expression of TGF-β1 and CTGF of hepatic fibrosis in rats [J]. China Journal of Modern Medicine. 2010;15:010.

[67] LIU Z-g, LI X-l, WENG L-d, LIU Q, ZHU H-x, HUANG Z-g. Research Progress in Pharmacological Effects of Silymarin. Journal of Liaoning University of Traditional Chinese Medicine 2012; 10: 036.

[68] Yang CH, Ting WJ, Shen CY, *et al*. SHSST‐cyclodextrin complex inhibits TGF‐β/Smad3/CTGF to a greater extent than silymarin in a rat model of carbon tetrachloride‐induced liver injury. Mol Med Rep 2015; 12(4): 6053-9.

[69] Zheng S, Chen A. Curcumin suppresses the expression of extracellular matrix genes in activated hepatic stellate cells by inhibiting gene expression of connective tissue growth factor. Am J Physiol Gastrointest Liver Physiol 2006; 290(5): G883-G93.

[70] O'Connell M, Rushworth S. Curcumin: potential for hepatic fibrosis therapy? Br J Pharmacol 2008; 153(3): 403-5.

[71] Chen A, Zheng S. Curcumin inhibits connective tissue growth factor gene expression in activated hepatic stellate cells *in vitro* by blocking NF-κB and ERK signalling. Br J Pharmacol 2008; 153(3): 557-67.

[72] Deng Y-T, Chen H-M, Cheng S-J, Chiang C-P, Kuo MY-P. Arecoline-stimulated connective tissue growth factor production in human buccal mucosal fibroblasts: Modulation by curcumin. Oral Oncol 2009; 45(9): e99-e105.

[73] Chuang S-E, Cheng A-L, Lin J-K, Kuo M-L. Inhibition by curcumin of diethylnitrosamine-induced hepatic hyperplasia, inflammation, cellular gene products and cell-cycle-related proteins in rats. Food Chem Toxicol 2000; 38(11): 991-5.

[74] Blakemore LM, Boes C, Cordell R, Manson MM. Curcumin-induced mitotic arrest is characterized by spindle abnormalities, defects in chromosomal congression and DNA damage. Carcinogenesis 2012.

[75] Georgopoulos NT, Steele LP, Thomson MJ, Selby PJ, Southgate J, Trejdosiewicz LK. A novel mechanism of CD40-induced apoptosis of carcinoma cells involving TRAF3 and JNK/AP-1 activation. Cell Death Differ 2006; 13(10): 1789-801.

[76] England H, Summersgill HR, Edye ME, Rothwell NJ, Brough D. Release of interleukin-1alpha or interleukin-1beta depends on mechanism of cell death. J Biol Chem 2014; 289(23): 15942-50.

[77] Wann AK, Knight MM. Primary cilia elongation in response to interleukin-1 mediates the inflammatory response. Cell Mol Life Sci 2012; 69(17): 2967-77.

[78] Edwards SK, Moore CR, Liu Y, Grewal S, Covey LR, Xie P. N-benzyladriamycin-14-valerate (AD 198) exhibits potent anti-tumor activity on TRAF3-deficient mouse B lymphoma and human multiple myeloma. BMC cancer 2013; 13(1): 481.

[79] Hacker H, Tseng PH, Karin M. Expanding TRAF function: TRAF3 as a tri-faced immune regulator. Nat rev Immunol 2011; 11(7): 457-68.

[80] Berbari NF, Kin NW, Sharma N, Michaud EJ, Kesterson RA, Yoder BK. Mutations in Traf3ip1 reveal defects in ciliogenesis, embryonic development, and altered cell size regulation. Dev biol. 2011;360(1):66-76.

[81] Wann AK, Chapple JP, Knight MM. The primary cilium influences interleukin-1beta-induced NFkappaB signalling by regulating IKK activity. Cell signal 2014; 26(8): 1735-42.

[82] Sinha SK, Zachariah S, Quinones HI, Shindo M, Chaudhary PM. Role of TRAF3 and -6 in the activation of the NF-kappa B and JNK pathways by X-linked ectodermal dysplasia receptor. J Biol Chem 2002; 277(47): 44953-61.

[83] Deguchi A. Curcumin targets in inflammation and cancer. Endocr Metab Immune Disord Drug Targets 2015; 15(2): 88-96.

[84] Karimian MS, Pirro M, Majeed M, Sahebkar A. Curcumin as a natural regulator of monocyte chemoattractant protein-1. Cytokine & Growth Factor Reviews 2017; 33(Supplement C): 55-63.

[85] Shehzad A, Qureshi M, Anwar MN, Lee YS. Multifunctional Curcumin Mediate Multitherapeutic Effects. J Food Sci 2017; 82(9): 2006-15.

[86] Kasi PD, Tamilselvam R, Skalicka-Woźniak K, *et al*. Molecular targets of curcumin for cancer therapy: an updated review. Tumour Biol 2016; 37(10): 13017-28.

[87] Feng T, Wei Y, Lee RJ, Zhao L. Liposomal curcumin and its application in cancer. Int J Nanomedicine 2017; 12: 6027-44.

[88] Teymouri M, Barati N, Pirro M, Sahebkar A. Biological and pharmacological evaluation of dimethoxycurcumin: A metabolically stable curcumin analogue with a promising therapeutic potential. J Cell Physiol 2018; 233(1): 124-40.

[89] Zhang L, Zong H, Lu H, Gong J, Ma F. Discovery of novel anti-tumor curcumin analogues from the optimization of curcumin scaffold. Med Chem Res 2017; 26(10): 2468-76.